Mixed-state parameters and vortex pinning in single-crystalline K_3C_{60} fullerene superconductors

V. Buntar, F. M. Sauerzopf, and H. W. Weber
Atominstitut der Österreichischen Universitäten, Schüttelstr. 115, A-1020 Wien, Austria

J. E. Fischer
Department of Materials Science and Engineering and Laboratory for Research on the Structure of Matter, University of Pennsylvania, Philadelphia, Pennsylvania 19104

H. Kuzmany and M. Haluska
Institut für Materialphysik, Universität Wien, Strudlhofgasse 4, A-1090 Wien, Austria

(Received 11 April 1997)

We report on detailed magnetic investigations of big K_3C_{60} single crystals with sizes of ~ 1 mm. The samples were characterized by x-ray analysis, neutron diffraction, and ac magnetization measurements. The temperature dependence of the upper and lower critical fields was obtained, the latter by the trapped magnetic-moment method. The coherence length and the penetration depth at $T=0$ and close to the transition temperature were evaluated. The magnetic field and the temperature dependence of the critical current density were studied and the irreversibility lines determined. Long-term magnetic relaxation, measured in a wide range of temperatures and magnetic fields, allowed us to obtain the temperature dependence of the relaxation rate and the flux creep activation energy at different magnetic fields. The influence of sample inhomogeneities on all these properties was investigated. The results are compared to those obtained on powder and polycrystalline samples. [S0163-1829(97)03145-7]

I. INTRODUCTION

Soon after the production of bulk quantities of fullerenes,[1] superconductivity was discovered in alkali-metal-doped C_{60}.[2,3] The transition temperatures of these materials are much higher than those of conventional superconductors, the highest transition temperature under normal pressure being $T_c=33$ K in $RbCs_2C_{60}$.[4] The first measurements of the upper[5,6] and the lower[5,7] critical fields in K_3C_{60} and Rb_3C_{60} established that alkali-doped fullerenes were type-II superconductors, and that their main superconducting parameters, the Ginzburg-Landau parameter κ, the penetration depth λ, the coherence length ξ, and the critical fields H_{c1} and H_{c2}, were similar to those of the high-T_c oxides.

However, the exact values of these parameters, obtained from different experiments, vary widely from sample to sample (see for details Ref. 8, Table I). For instance, the upper critical field was reported to be between 17 T (Ref. 9) and 49 T (Ref. 5) for K_3C_{60} and between 40 T (Ref. 10) and 78 T (Ref. 7) for Rb_3C_{60}. This led to uncertainties in the magnitude of the coherence length, which was reported to be between 2 nm (Ref. 11) and 4.5 nm (Ref. 12) and between 2 nm (Ref. 7) and 3 nm (Ref. 10) for K_3C_{60} and Rb_3C_{60}, respectively. The difficulties appeared mainly because powder samples or very small crystals of badly defined stoichiometry were investigated.

An even worse situation was encountered with the determination of the lower critical field. It was accepted at the beginning that H_{c1} at zero temperature was of the order of 10–16 mT for both K_3C_{60} and Rb_3C_{60}, leading to penetration depths of the order of 220–280 nm. These data for H_{c1} were usually obtained from the fields at which the first deviation from linearity in $M(H)$ appeared. However, none of the magnetization data for fullerene materials showed good linearity. Measured at rather big magnetic field intervals (~ 0.5 mT), $M(H)$ usually showed a smooth positive and in some experiments even a negative curvature.[13] Other methods very often led to values of $H_{c1}(0)$, which were much smaller than 10 mT,[14–16] or to penetration depths of the order of 500 nm (Refs. 17 and 18) and larger.[19] These small values of the lower critical field were usually attributed to sample imperfections, especially to weak links, etc.

Because of these uncertainties, measurements on big crystalline samples of good quality are clearly needed to decide whether the parameters obtained from experiment are characteristic of the bulk material or of weak links. Only this will allow us to establish the true intrinsic superconducting parameters.

In addition, investigations of flux pinning and of pinning-related properties, such as the critical current density J_c, the irreversibility line, the activation energy, etc., are of great interest. Although several years have passed since the discovery of superconductivity in fullerenes,[2] only a few results on flux pinning[20,21] and magnetic relaxation[6,22–24] were published. In Refs. 6 and 23, the flux creep activation energy was estimated to be of the order of 10^{-2} eV. However, it should be pointed out that all of the early measurements were performed on powder samples, where the magnetic relaxation usually did not show a logarithmic time dependence.[22] Even some peaks were observed in the $M(t)$ curves during short-term relaxation.[24] This behavior could be connected to an intergranular interaction between grains in powder samples as well as to weak links, which may exist in samples of poor quality.

In this paper, we report on detailed magnetic investigations of K_3C_{60} single crystals with volumes between 1 and

TABLE I. Main parameters of K_3C_{60} single crystals.

Sample	Weight (mg)	Volume (mm^3)	Structure	Shielding fraction	T_c (K)
K1	1.8	0.9	mosaic 5°, + pure C_{60}	25%	19.2
K2	1.8	0.9	mosaic 5°, + pure C_{60}	30%	19.2
K3	4	2	mosaic 5°, + pure C_{60}	65%	19.6
K4	11.2	5.6	mosaic 3°, no pure C_{60}	100%	19.2
K5	4.8	2.4	mosaic 3°, no pure C_{60}	100%	19.2
K6	2.1	1.1	mosaic 3°, no pure C_{60}	100%	19.2

6 mm^3, i.e., where their dimensions are much larger than the penetration depth of this material. Samples are well characterized by x-ray and neutron diffraction as well as ac and dc magnetic measurements. Measurements of the main superconducting parameters, such as the critical fields and the characteristic lengths, as well as of the pinning related parameters were carried out. We investigated samples of different quality with various degrees of nonsuperconducting imperfections, in order to determine the influence of these factors on the superconducting properties.

II. EXPERIMENT

The K_3C_{60} crystals were obtained by doping C_{60} single crystals using potassium azide, KN_3, or K metal as a source of potassium. Details of the sample preparation are given elsewhere.[25] The K_3C_{60} crystals are of different quality with shielding fractions (x_{sh}) from 25% up to 100%. The best crystals, with $x_{sh}=100\%$, have good K_3C_{60} stoichiometry and x-ray diffraction does not show any evidence of other phases, such as KC_{60} or C_{60}. The crystals with $x_{sh}<100\%$ usually contain some amount of potassium deficient components (pure or underdoped C_{60}) which can be observed, for instance, by neutron diffraction. For example, an intensity ratio of ~ 1.3 between the (220) and (311) intensities was observed on sample K2 ($x_{sh}=30\%$), which is intermediate between the expected 1.8 and 0.64 for C_{60} and K_3C_{60}, respectively. All the crystals, independently of the volume or the shielding fraction, have a mosaic structure with misorientations from 3° to 5°, which appears during the doping procedure. The main characteristics of the samples are presented in Table I.

In powder samples the grain size ($\sim 1\ \mu$m) is comparable to the penetration depth of K_3C_{60},[26] which is 800 nm at zero temperature. This strongly affects a large number of experimental data on powders, but is of no significance for our large samples. On the other hand, the spread in x_{sh} of our crystals allows us to investigate the influence of the sample impurities on the measured quantities.

The magnetic measurements were performed in two superconducting quantum interference device (SQUID) magnetometers. One of them is a commercial Quantum Design SQUID magnetometer equipped with a superconducting 1 T magnet. This device has a very high sensitivity, which is mainly achieved by an environmental magnetic shield attenuating stray fields. Moreover, a special low-field option allows us to hold the residual field in the magnet at a very low level ($<5\times10^{-8}$ T). Due to these options, very precise measurements of the trapped magnetization and very small increments of the external magnetic field can be achieved. This device was used for ac measurements, measurements of the trapped magnetization to determine H_{c1}, and measurements of the temperature- and magnetic-field-dependent magnetization to obtain H_{c2}, x_{sh}, J_c, and H_{irr}. Also, magnetic relaxation measurements were carried out.

The second device, a noncommercial SQUID magnetometer, based on a S.H.E. variable temperature system (VTS), is equipped with an 8 T magnet and was used to measure the magnetization in high magnetic fields as a function of temperature (for the determination of H_{c2}) and magnetic field (determination of J_c and H_{irr}).

III. dc AND ac CHARACTERIZATION

The temperature dependence of the dc magnetic susceptibility [$\chi=m/(H_{ext}V)$], where m is the magnetic moment, H_{ext} is the external field, and V is the sample volume, is measured in order to obtain the transition temperature T_c and the shielding and Meissner (x_M) fractions. Measurements of both zero-field-cooled (ZFC) and field-cooled (FC) curves are performed in a magnetic field of 0.1 mT. The results of these measurements are given in Table I. Both branches (ZFC and FC) are smooth without any steps (Fig. 1). The critical temperatures of the samples, obtained from the crossing point of the extrapolations of the linear part of the FC magnetization $M(T)$ in the superconducting state and the small normal-state magnetization, range from 19.2 to 19.6 K. For three specimens, K4–K6, the experimentally determined slope in the Meissner phase coincides with that calculated from approximated demagnetizing factors.[27] K4–K6 are denoted further on as samples with 100% shielding fraction, which is confirmed by the structural analysis discussed in the previous section, and by the ac characterization, which will be discussed below. The other samples (K1, K2, and K3)

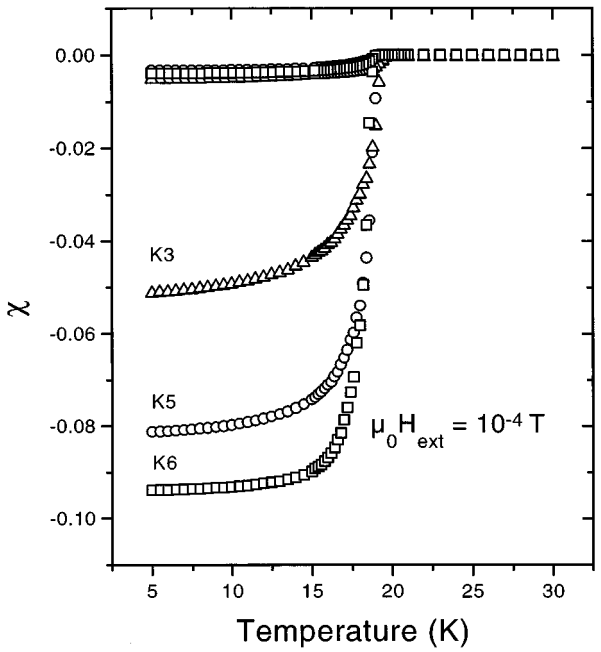

FIG. 1. Temperature dependence of the magnetic susceptibility of K3 (triangles), K5 (circles), and K6 (squares).

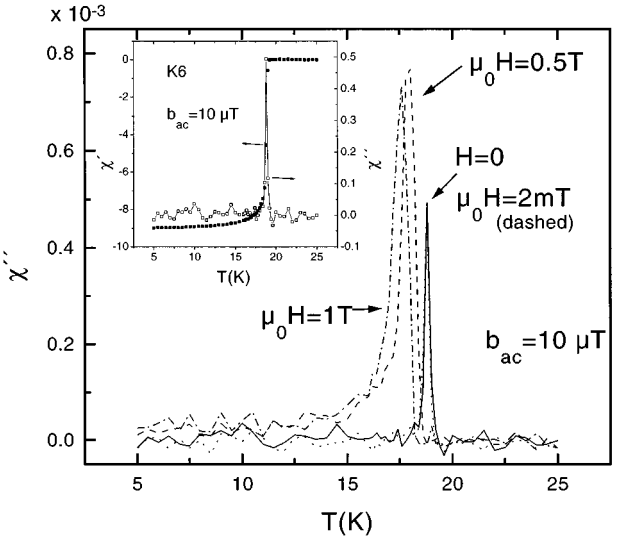

FIG. 2. Temperature dependence of the imaginary part of the susceptibility at an ac field amplitude $b_{ac}=10^{-5}$ T (frequency 31 Hz) and dc fields of 0 (solid line), 2 mT (dotted line), 0.5 T (dashed line), and 1 T (dash-dotted line). The inset shows the real and the imaginary parts of the susceptibility as a function of temperature ($b_{ac}=10^{-5}$ T, and $\mu_0 H=0$).

exhibit 25%, 30%, and 65% shielding, respectively. These results are in a good agreement with the structural characteristics of the samples.

The FC magnetic susceptibility is small for all samples and indicates a Meissner effect from 5% to 10%. Such insignificant flux expulsion is connected to strong pinning, which is, most probably, due to structural defects like inhomogeneities, the mosaic structure, surface imperfections, etc.

For the samples with 100% shielding fraction, the experimental demagnetizing factor D was obtained from $M(H)$ and $M(T)$ ZFC measurements. We assume that complete flux exclusion prevails and fit the slope of the straight $M(H)$ line to $M=-H/(1-D)$, which leads to the demagnetizing factors ($D\simeq 0.18$, 0.6, and 0.14, for K4, K5, and K6, respectively). For samples with $x_{sh}<100\%$, we cannot use the experimental values and have to rely on approximate calculations.

Because of the short coherence length in K_3C_{60} [$\xi\sim 3$ nm (Ref. 5)], the mosaic structure, which is observed in all the samples, could lead to the presence of weak links due to the mismatch between neighboring blocks of different orientation, a disturbance of the structure at the surface of the blocks or impurity phases between the grain boundaries. The latter is the most important factor for samples with imperfect stoichiometry (K1, K2, and K3). In order to check if our samples can be treated as bulk superconductors, ac measurements were performed in dc fields between 0 T and 1 T, using ac fields between 1×10^{-7} T and 5×10^{-4} T, and temperatures from 5 K to T_c.

ac measurements are a very powerful tool for characterizing specimens and for discriminating between inter- and intragranular properties. With decreasing temperature the material becomes superconducting at T_c. However, the weak links are still resistive. Therefore, in the temperature range between T_c and the temperature T_{c1}, where the weak links become able to carry a supercurrent, the shielding currents only flow within the grains, whereas the sample is fully shielded at lower temperatures. According to a straightforward Bean model analysis, this leads to a multiple-peak structure in the $\chi''(T)$ dependence, in contrast to a sharp single peak for a sample without grain boundaries.

ac techniques were already applied to fullerenes by different groups[9,28,29] and the results[9] showed evidence for the existence of inter- and intragrain dissipation mechanisms, because two peaks in the temperature dependence of the imaginary part of the susceptibility were clearly seen.

The temperature dependence of the real and imaginary parts of the ac susceptibility is shown in the inset of Fig. 2 for sample K6. The sharp drop of χ' shows the transition to the superconducting state at a temperature T_c, which corresponds to that obtained from dc measurements. The peak in $\chi''(T)$ is very sharp and close to the critical temperature. $\chi''(T)$ for various magnetic fields up to 1 T is shown in Fig. 2. As expected, the peak moves to lower temperatures with increasing H_{ext}. It becomes broader, but is still sharp.

In contrast to the samples with 100% shielding fraction, samples K1, K2, and K3 exhibit a much more complicated structure of $\chi''(T)$. In Fig. 3, $\chi''(T)$ is compared for samples K3 and K6. The same sharp peak as for K6 at $T=T_c$ is also observed for K3. However, several other peaks can clearly be seen at lower temperatures. These peaks are attributed to the dissipation due to weak links. This granularity appears in the samples because of nonsuperconducting impurities (undoped C_{60} or probably KC_{60}) between superconducting grains.

The ac measurements prove that there is no granularity for current flow in the pure samples with 100% superconducting fraction, although a mosaic structure was observed. The properties of these samples may be compared to those of melt-textured high-T_c superconductors, which also exhibit

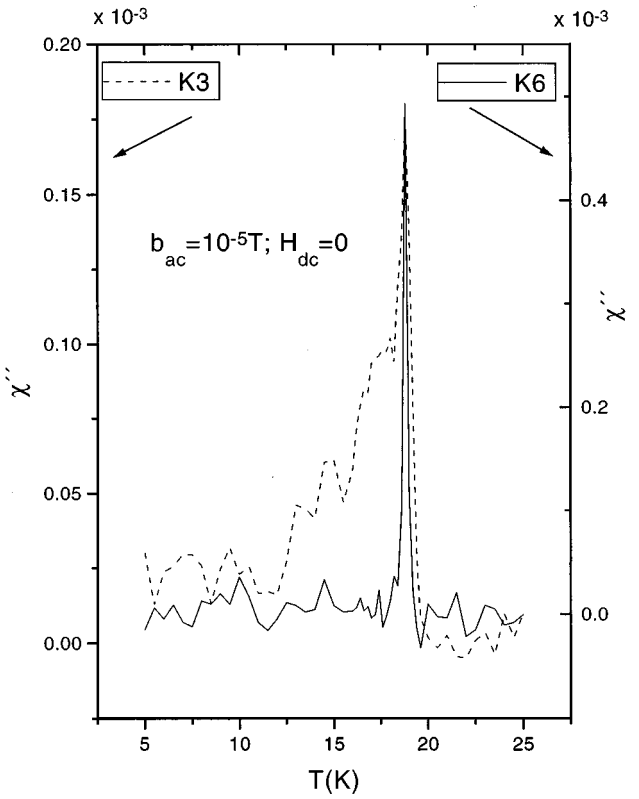

FIG. 3. Imaginary part of the susceptibility vs temperature at $b_{ac}=10^{-5}$ T and $\mu_0 H=0$ for K6 (solid line) and K3 (dashed line).

small misorientations between grains, but no granularity for the superconducting current flow.

IV. CRITICAL FIELDS AND CHARACTERISTIC LENGTHS

The temperature dependence of the upper critical magnetic field was obtained from FC curves. H_{c2} was determined in these experiments from the crossing point of extrapolations of the linear part of the magnetization $M(T)$ in the superconducting state and the small normal-state magnetization, neglecting fluctuation effects.

The $H_{c2}(T)$ dependence of samples K1 (25% shielding fraction) and K6 (100% shielding fraction) in fields up to 8 T is shown in Fig. 4. It is linear at these temperatures with a slope $\delta\mu_0 H_{c2}/\delta T=-2.1$ T/K, and the same for both samples. The slope is consistent with data obtained by other groups (1.34 T/K$<\mu_0 H_{c2}/T<$5.5 T/K: see Table I in Ref. 8). Using the standard theory of Werthamer, Helfand, and Hohenberg (WHH),[30] the upper critical field at zero temperature $H_{c2}(0)$ can be evaluated from the relation (clean limit)

$$\mu_0 H_{c2}(0)=-0.69 T_c \frac{\delta\mu_0 H_{c2}}{\delta T}. \quad (1)$$

We obtain $\mu_0 H_{c2}(0)=28$ T [as compared to 17 T $<\mu_0 H_{c2}(0)<$49 T: see Table I in Ref. 8]. The Ginzburg-Landau relation

$$\mu_0 H_{c2}=\frac{\Phi_0}{2\pi\xi^2} \quad (2)$$

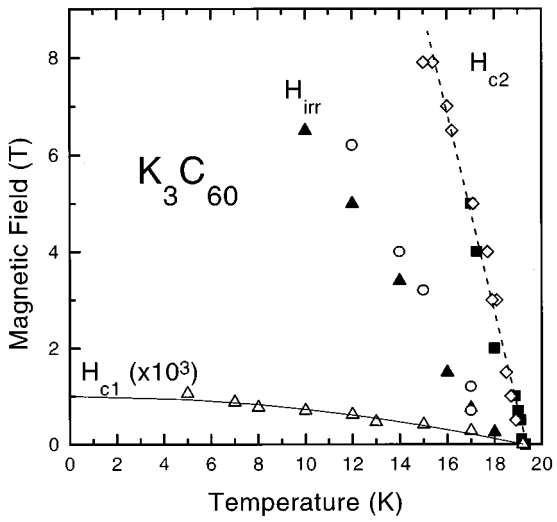

FIG. 4. H-T phase diagram of K_3C_{60}. Open symbols correspond to K6, solid symbols to K1. (The values of the lower critical field are multiplied by a factor of 1000.)

(where $\Phi_0=h/2e$ is the flux quantum and ξ is the coherence length) leads to $\xi(T=0)=3.4$ nm (compared to 2 nm$<\xi<$4.5nm; Table I in Ref. 8). These values are very close to those obtained by Johnson *et al.*[10] on powder samples. The slope of -2.1 T/K is close to that obtained by Boebinger *et al.*[28] However, due to a strange enhancement of the upper critical field in their experiments at low temperatures, the value of $H_{c2}(0)$ in Ref. 28 was slightly higher than our extrapolated one, leading to a smaller coherence length.

The upturn of $H_{c2}(T)$ at temperatures very close to T_c, which was observed in almost all experiments on fullerene superconductors, is another interesting effect which we would like to discuss here. Various explanations were suggested. The authors of Ref. 5 consider this deviation to be a consequence of slight variations in the local T_c, while in Ref. 9 the effect is attributed to a crossover from three to two dimensionality. One explanation[31] is that the upturn at low fields might be due to sample imperfections. In order to check this, we performed detailed measurements of the upper critical field close to T_c in crystals of different quality with shielding fractions between 25% and 100%. The same effect is found in all samples, and no influence of the imperfections can be detected (Fig. 5). We suggest that the upturn is a consequence of the anisotropy of Fermi surface in the fullerene superconductors.[32] Strong effects of the anisotropy on the magnetic properties of conventional superconductors, specifically on H_{c2}(T), are well known.[33]

As discussed in the Introduction, the determination of the lower critical field by different methods, such as the first deviation from the linear $M(H)$ dependence,[5,7] from Bean's relation $\Delta M\sim H^2$,[15] from the reversible part of $M(H)$ at intermediate and high magnetic fields,[34,35] from the measurements of irreversibility in $M(T)$ at low fields,[16] etc., led to a large scatter of data. Small lower critical fields (below 5 mT) were usually attributed to breaking of the Josephson junctions between grains. However, H_{c1} was usually significantly decreasing with increasing precision of the method employed.

In order to avoid these problems, we obtained the lower

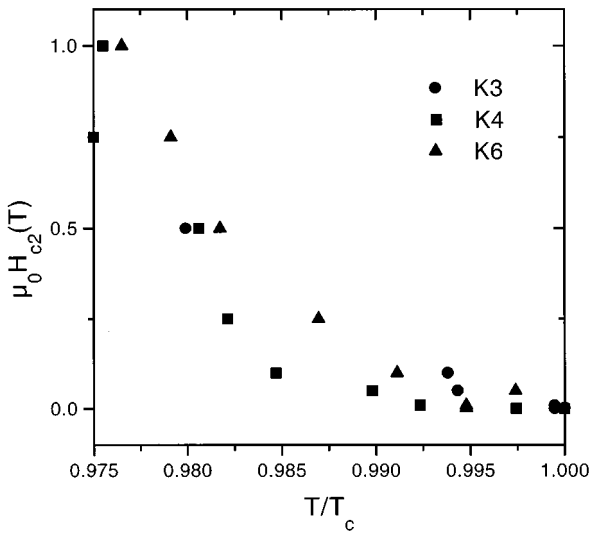

FIG. 5. Temperature dependence of the upper critical field close to T_c for samples K3 (circles), K4 (squares), and K6 (triangles).

critical field from measurements of the trapped magnetization m_{tr}.[36,37] This method is very sensitive due to the cancellation of the linear part of the magnetization. As shown for the cuprates, the trapped magnetization could clearly be observed at fields, where no deviation from linearity of $M(H)$ was visible.[36] Furthermore, this is a direct measurement of the field penetrated into the sample and does not require any fitting parameters.

The measurement of m_{tr} proceeds as follows. The sample is cooled down from $T>T_c$ to the desired temperature in zero external magnetic field. After temperature stabilization, the magnetic moment m_1 is measured. After this first measurement, a certain magnetic field H_a is applied and kept fixed for some time (usually for 5–20 s). Then the magnetic field is reduced to zero and the magnetic moment m_2 measured. The trapped magnetic moment is $m_{tr}=m_2-m_1$. Afterwards, the sample is heated up to $T>T_c$. These cycles are repeated, the value of the applied field H_a being higher each time than during the previous cycle, with step increments of 10–50 μT. The principle of this experiment is based on the fact that magnetic fields do not penetrate the sample for $H_a/(1-D)<H_{c1}$ and that the magnetic moment measured before and after the application of H_a is the same. However, as soon as $H_a/(1-D)$ exceeds H_{c1}, m_2 should be smaller than m_1 due to the trapped magnetic flux, which is pinned in the sample, and $m_{tr}=m_2-m_1>0$.

The temperature dependence of H_{c1} obtained with this method is shown in Fig. 4. (Because of the smallness of H_{c1} compared to H_{c2}, the lower critical fields in Fig. 4 are multiplied by a factor of 1000.) The smallness of $H_{c1}(0)=1$ mT cannot be attributed to the breaking of weak links between grains because of the good quality of the sample and the absence of granularity confirmed by the ac measurements. In order to find out if granularity affects $H_{c1}(T)$, we also performed measurements of the trapped magnetization on samples with granularity (see Fig. 3). We find that $H_{c1}(0)$ is the same in all samples with x_{sh} between 25% and 100% $[H_{c1}(0)=1.2\pm0.3$ mT]. In addition, the trapped magnetization is proportional to the square of the magnetic field, which is the case for fields penetrating the bulk, and not between grains.[36] Therefore, we can definitely state that the lower critical field of K_3C_{60} at zero temperature is not higher than 1.2 mT, and that the smallness of $H_{c1}(0)$ is not connected to the breaking of Josephson junctions or weak links, but is an intrinsic property of this material.

The penetration depth λ at zero temperature, obtained from the equation

$$\mu_0 H_{c1}=\frac{\Phi_0}{4\pi\lambda^2}\ln\kappa, \tag{3}$$

with $\xi(0)=3.4$ nm, is $\lambda(0)=870$ nm, and, therefore, the Ginzburg-Landau (GL) parameter for K_3C_{60} is $\kappa=256$. As far as we know, this is the highest GL parameter of any type-II superconductor at present. (The mixed-state parameters obtained for each sample are listed in Table II.)

This result is in a very good agreement with optical measurements.[19] Considering the indirect evaluation procedure employed to obtain λ from magnetization and muon spin relaxation (μSR) measurements,[17,18] the difference between these results is not very large. This difference could be related to the fact that the μSR measurements were done on powder samples with an average grain radius r of the order of the penetration depth. The distribution of the magnetic field (which is actually measured by μSR) in grains with $r\simeq\lambda$ is effectively ''cut off'' at least at half of the amplitude. Therefore, the effective ''μSR penetration depth'' should be shorter than the real one. On the other hand, the distribution of the magnetic field in a *system* of vortices with an intervortex distance much shorter than the penetration depth could be calculated more carefully. However, some models have to be used for such a calculation, which may lead to a discrepancy between results by a factor of 2. Not enough details about the calculation procedure are given in Refs. 17 and 18. Therefore, we cannot give an exact answer as to why the values of the penetration depth found from these mea-

TABLE II. Mixed-state parameters of K_3C_{60} single crystals.

Sample	H_{c1} (mT)	$\delta H_{c2}/\delta T$ (T/K)	H_{c2} (T)	ξ (nm)	λ (nm)	κ
K1	1.5	−2.1	28	34.3	770	225
K3	1.25	-	-	-	-	-
K4	-	−2.13	28.2	34.2	-	-
K5	1.25–1.5	−2.25	29.8	33.25	744–855	224–257
K6	0.9–1	−2.1	28	34.3	960–1020	278–297
Average	1.27	−2.145	28.5	34.0	853	251

surements are smaller than ours and those evaluated from optical measurements. Also, one has to bear in mind that all the procedures to obtain λ strongly depend on underlying models. Under this aspect, the observed discrepancies are considered to be rather small.

Because the average grain radius r of powder samples is comparable to the penetration depth λ, the grains are penetrated by magnetic flux at all fields. Therefore, a correction $r/\lambda(0)$ has to be included to determine the superconducting volumes. This was done in Ref. 38 for Rb_3C_{60} powder. The authors fitted theoretical curves to the experimental data of Ref. 39 using three different theories for $\lambda(T)$, Ginzburg-Landau theory, BCS theory, and the two-fluid model. In the temperature range $5\ \mathrm{K}=0.17T_c \leqslant T \leqslant 0.71T_c=20\ \mathrm{K}$ the two-fluid model was completely inappropriate, and the best fit was achieved with the Ginzburg-Landau temperature dependence

$$\lambda(T)=\lambda_{\mathrm{GL}}(0)[1-(T/T_c)]^{-1/2}, \tag{4}$$

which gave an increase of the superconducting fraction compared to the experimental data by a factor of 2 $[r/\lambda(0)=4.8]$. The BCS dependence

$$\lambda(T)=\lambda_{\mathrm{GL}}(0)[1-(T/T_c)^2]^{-1/2}, \tag{5}$$

resulted in a much higher increase of the superconducting fraction, by factor of 7. The authors, assuming the penetration depth to be of the order of 200–300 nm, found this result unacceptable. However, in the light of our data for λ, r $(\sim 1\ \mu\mathrm{m})/\lambda(\sim 0.87\ \mu\mathrm{m}) \simeq 1$, the BCS result seems to be much better.

From the experimentally obtained temperature dependence of the upper critical field in the range from 15 K up to T_c, $\xi(T)$ is evaluated from Eq. (2). From $\xi(T)$ and using the data of $H_{c1}(T)$ in the same temperature range, we obtain the temperature dependence of the penetration depth from Eq. (3). $\xi(T)$ and $\lambda(T)$ are shown in Fig. 6. We fitted our experimental data to Ginzburg-Landau theory [Eq. (4)], BCS theory [Eq. (5)], and the two-fluid model,

$$\lambda(T)=\lambda_{\mathrm{GL}}(0)[1-(T/T_c)^4]^{-1/2}, \tag{6}$$

using $\lambda_{\mathrm{GL}}(0)$ and $\xi(0)$ as fit parameters. All theories describe both $\xi(T)$ and $\lambda(T)$ well and, because there is almost no significant difference between them, only the BCS dependence is shown in Fig. 6. However, this is only true in the temperature range shown in Fig. 6, since the fit parameters $\xi_{\mathrm{fit}}(0)$ and $\lambda_{\mathrm{fit}}(0)$ are largely different. Both the coherence length and the penetration depth at zero temperature, obtained from the BCS fit [$\xi_{\mathrm{fit}}(0)=3.8$ nm and $\lambda_{\mathrm{fit}}(0)=887$ nm], agree well with those obtained from $H_{c2}(0)$ and $H_{c1}(0)$, $\xi(0)=3.4$ nm and $\lambda_{\mathrm{GL}}(0)=870$ nm. The Ginzburg-Landau fit gives $\xi_{\mathrm{fit}}(0)=2.85$ nm, which is also close, but is by the factor of 1.2 smaller for the penetration depth $\lambda_{\mathrm{fit}}(0)=644$ nm. The fit parameters, obtained from the two-fluid model, $\xi_{\mathrm{fit}}(0)=4.9$ nm and $\lambda_{\mathrm{fit}}(0)=1185$ nm, do not agree at all with the above results.

We conclude that the best fit for $\xi(T)$ and $\lambda(T)$ is the BCS dependence and that Ginzburg-Landau theory also describes the data reasonably well. The two-fluid model, in agreement with the results in Ref. 38, is found to be completely inappropriate.

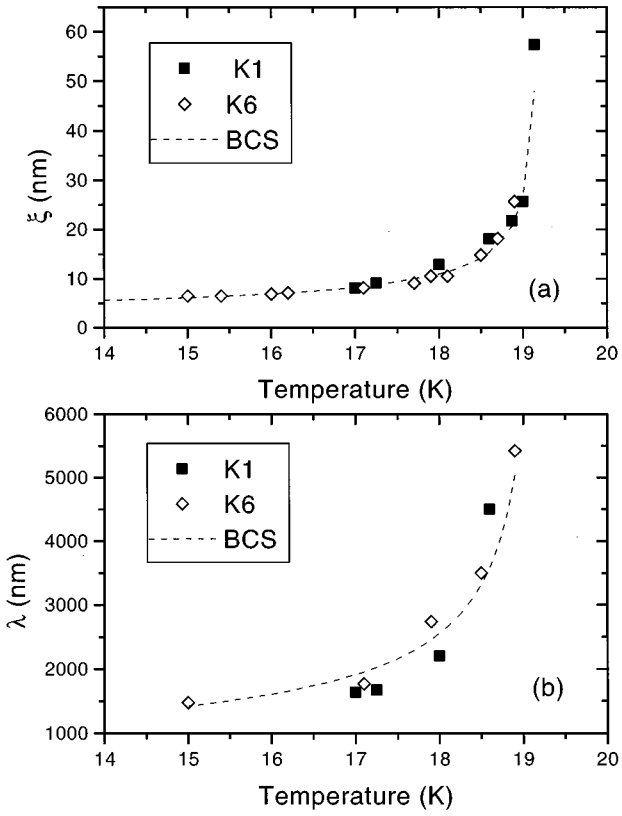

FIG. 6. The coherence length (a) and the penetration depth (b) vs temperature. Open symbols correspond to sample K6 and solid symbols to sample K1. The dashed line shows the BCS dependence with fit parameters $\xi_{\mathrm{fit}}(0)=3.8$ nm and $\lambda_{\mathrm{fit}}(0)=887$ nm.

V. CRITICAL CURRENT DENSITY AND IRREVERSIBILITY LINE

Measurements of $M(H)$ at various temperatures were performed in order to obtain the magnetic field and temperature dependence of the critical current density $J_c(H,T)$ and the irreversibility line $H_{\mathrm{irr}}(T)$. According to Bean's critical-state model,[40] J_c can be determined from the hysteresis loop by the equation

$$J_c=3\frac{M_+-M_-}{R}, \tag{7}$$

where M_+ and M_- (in $\mathrm{A\ m^{-1}}$) denote the magnetization measured in increasing and decreasing fields at a certain magnetic field, and R is the sample radius.

While R can be approximated using the sample size for single crystals, it is determined from the grain size in powders. Boss *et al.*[41] investigated the J_c dependence on the size of their samples, R, in the range from 1 μm to 300 μm. They observed that the widths of the hysteresis loops were independent of sample size, i.e., $J_c \sim 1/R$, implying that the mean radius R of the shielding currents must be smaller than the smallest radius of their samples, i.e., $R \sim 1\ \mu$m, the size of an individual grain.

This contradicts magnetization measurements performed by several groups on different samples for both K_3C_{60} and Rb_3C_{60}.[6,9,42,43] According to these results, the width of the hysteresis loops increases with sample size, although not

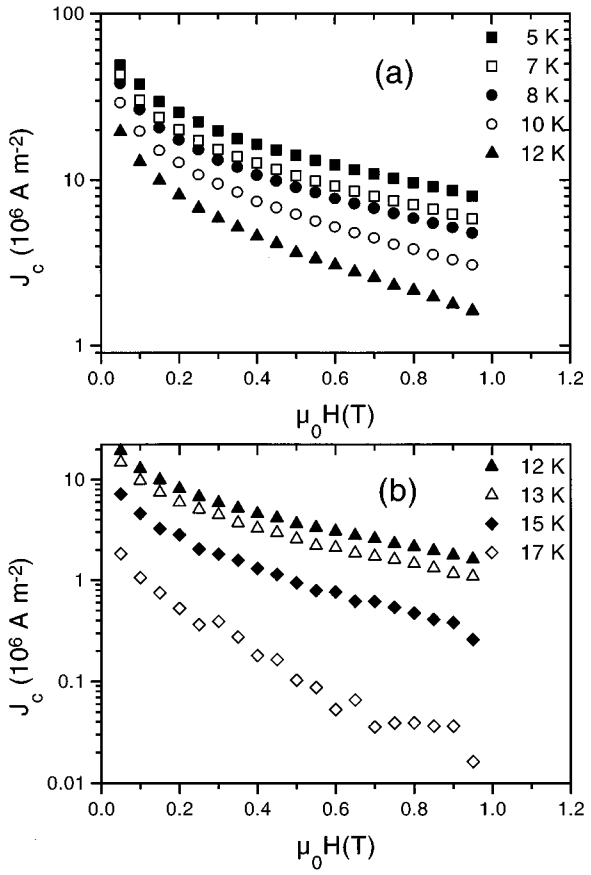

FIG. 7. Magnetic field dependence of the critical current density at fixed temperatures: (a) 5 K, 7 K, 8 K, 10 K, and 12 K, and (b) 12 K, 13 K, 15 K, and 17 K.

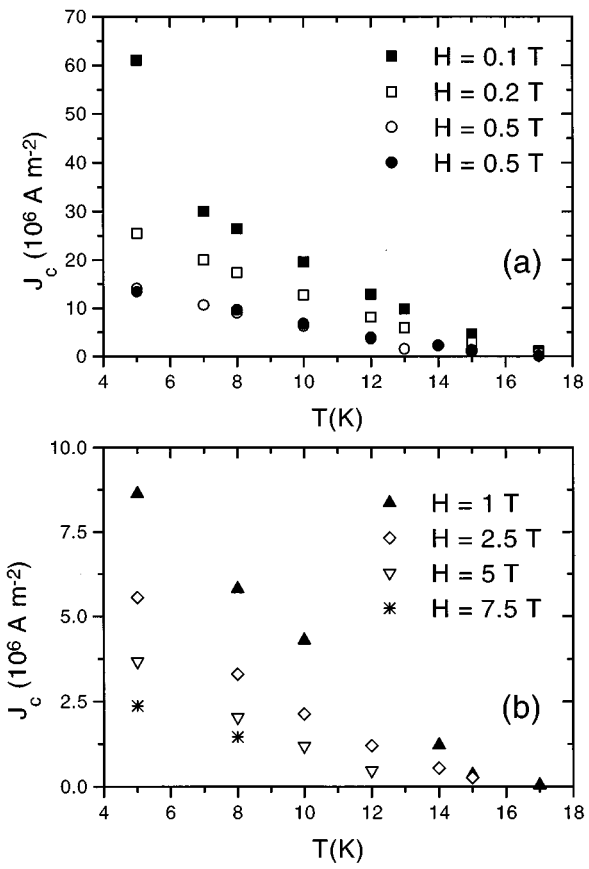

FIG. 8. Temperature dependence of the critical current density at fixed magnetic fields: (a) 0.1 T, 0.2 T, 0.5 T, and (b) 1 T, 2.5 T, 5 T, and 7.5 T.

proportionally. This can be explained by weaker pinning in single crystals compared to powder samples, due to the much smaller number of pinning centers in the more perfect structure of the crystals.

For the determination of the critical current density in sample K6 with $x_{sh}=100\%$, we use $R=1$ mm. We obtain that $J_c=6\times10^7$ A m^{-2} at T=5 K and $\mu_0 H=0.05$ T. This value is close to that obtained in Ref. 42 for 1-mm-sized K_3C_{60} and Rb_3C_{60} crystals and by a factor of 15 smaller than reported for Rb_3C_{60} in Ref. 43. This difference could again be connected to the quality of the crystals.

The magnetic field and temperature dependence of the critical current density obtained on sample K6 is shown in Figs. 7 and 8. The critical current density decreases smoothly with increasing magnetic field and temperature. If we compare these values to $YBa_2Cu_3O_7$ single crystals, which have the lowest anisotropy of all high-temperature superconductors, we find that J_c is significantly smaller (by about a factor of 100; see, e.g., Ref. 44). This cannot be explained at the moment, because the expected contribution of defects to flux pinning depends on H_c and ξ, both of which do not differ much from $YBa_2Cu_3O_7$, and because the size of the defects can hardly be much smaller than the lattice parameter and, therefore, has to be comparable to ξ.

We do not compare the absolute values of the critical current densities for samples with different shielding fractions, because we do not know the distribution of superconducting and nonsuperconducting regions in samples with $x_{sh}<100\%$, and, therefore, cannot correctly determine R. However, we find that the temperature and magnetic field dependence of the width of the hysteresis loops, which is proportional to J_c, has the same character for all samples.

In a wide field range, the magnetic field dependence of the inverse critical current density in all samples is found to be proportional to B as shown in Fig. 9. Similar results were previously observed on other superconducting compounds.[8,39] At higher temperatures the same general behavior is found, but J_c suddenly becomes smaller than the resolution of our experimental device at some characteristic value of the external magnetic field (Fig. 9).

The values of the critical current density before J_c drops to zero are still above the resolution limit of our device. The magnetic field dependence of J_c at $T=17$ K, shown in Fig. 7(b), ends with a plateau at $\mu_0 H\geqslant0.7$ T with $J_c\sim4\times10^3$ A m^{-2}. At this level of the experimental signal, ΔM is close to (but still slightly higher than) the standard deviations of the moments for each SQUID scan. These deviations are of the order of 5×10^{-10}–5×10^{-9} A m^2 and are rather high because of the presence of a quartz capsule. We consider this value of ΔM to be the resolution limit. It is shown (translated into J_c for sample K6) by the dashed line in Fig. 9.

From the characteristic magnetic fields, at which J_c sharply drops below the resolution limit of our device, we define the irreversibility field H_{irr}. The temperature depen-

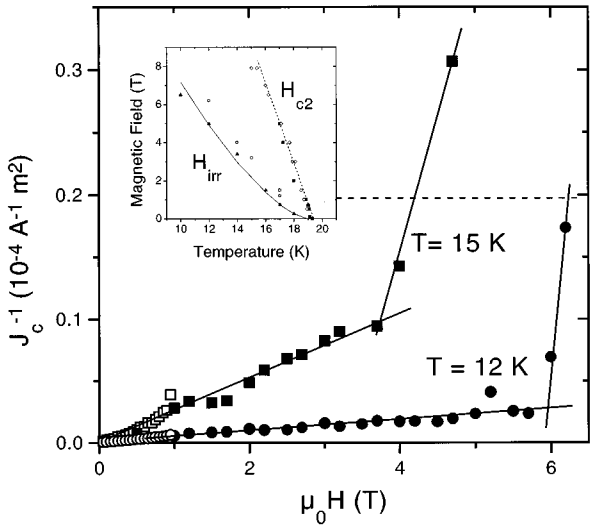

FIG. 9. Magnetic field dependence of the reciprocal critical current density at $T=15$ K (squares) and $T=12$ K (circles). Open symbols correspond to data obtained with the 1 T SQUID magnetometer; solid symbols correspond to data obtained with the 8 T SQUID magnetometer; The dashed line shows the resolution limit. The inset shows the irreversibility line, evaluated from $1/J_c \sim H$, for samples K1 (solid symbols) and K6 (open symbols).

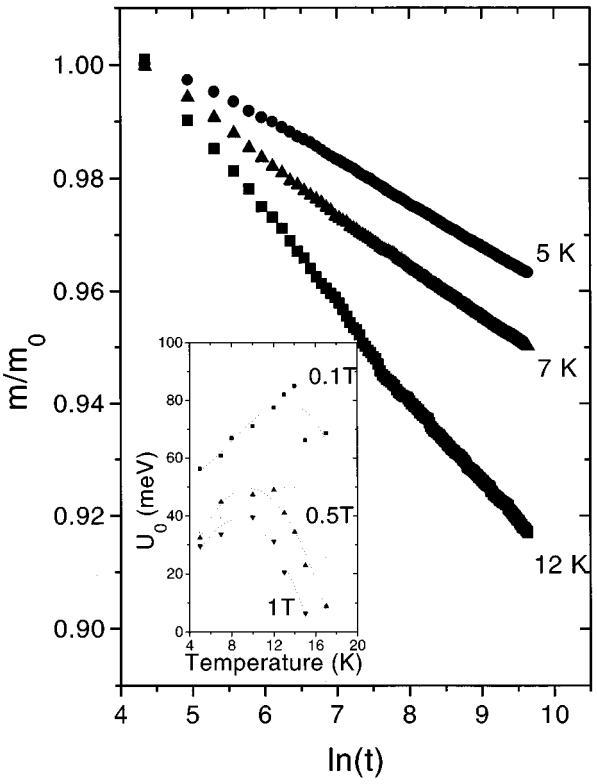

FIG. 10. Time-dependent magnetic moment m/m_0 at 5 K, 7 K, and 12 K. The inset shows the flux creep activation energy vs temperature at external fields of 0.1 T, 0.5 T, and 1 T.

dence of the irreversibility field (''irreversibility line'') obtained in this way for K1 and K6 is shown in the inset of Fig. 9. The irreversibility line follows the power law:

$$H_{\rm irr}=H_0\left(1-\frac{T}{T_c}\right)^m, \tag{8}$$

with $m=1.5$. Therefore, the irreversibility line can be described in terms of thermally activated flux flow,[45] but could also agree with vortex lattice melting.[46]

VI. MAGNETIC RELAXATION AND FLUX CREEP ACTIVATION ENERGY

The magnetic moment of an irreversible superconductor in an external magnetic field relaxes due to thermal activation of vortices. This phenomenon was often observed in high-T_c superconductors. It is interesting that fullerene superconductors with their much smaller transition temperatures exhibit comparable magnetic relaxation. The time dependence of the magnetic moment at different temperatures and external fields is an important feature of these superconductors and provides valuable information on the pinning potential for the vortices.

In this section we present experimental results of dc magnetic relaxation measurements for samples with different shielding fraction. The temperature range of these measurements extended from 5 K to $T_c \sim 19$ K, and the range of magnetic fields was $\mu_0 H_{c1} \ll 0.1$ T$\leq \mu_0 H \leq 1$ T$\ll \mu_0 H_{\rm irr}$. This range of external fields ensures complete flux penetration into the samples. The ramp rate of the magnetic field was approximately 28 mT/s and the same for all applied fields in our experimental window. The magnetic relaxation was recorded up to 5×10^4 s. The measurements were performed as follows. The specimen was cooled from $T=30$ K$>T_c$ down to $T<T_c$ in zero external field. After temperature stabilization, an external field was applied. The magnetization was monitored at fixed T and $H_{\rm ext}$. The first measurements were performed at $t_0 \sim 80$ s after field stabilization. Consecutive measurements were carried out every 60–63 s. The data in each group of samples, the impure (K1, K2, and K3) and the single grains (K4, K5, and K6), are very similar. In this paper we mainly show results on sample K1 and K6 representing sample groups with nonperfect and perfect stoichiometry, respectively.

The time-dependent magnetization of sample K6 at an external magnetic field 0.1 T and for temperatures from 5 K to 17 K is presented in Fig. 10. The relaxation process is logarithmic within our experimental time window. The creep rate $\delta M(t)/\delta \ln t$ decreases linearly with increasing temperature and extrapolates to zero at some $T_0 \sim 18.1$ K$<T_c$, which is the same for all external fields. The relaxation rate

$$S=\frac{1}{M}\frac{\delta M}{\delta \ln t}$$

(M is the initial value of the magnetization after the external field change) increases smoothly with increasing temperature at all fields and becomes larger with increasing field.

The temperature dependence of the flux creep activation energy, U_0, is obtained from the decay of the magnetization with the relationship[47]

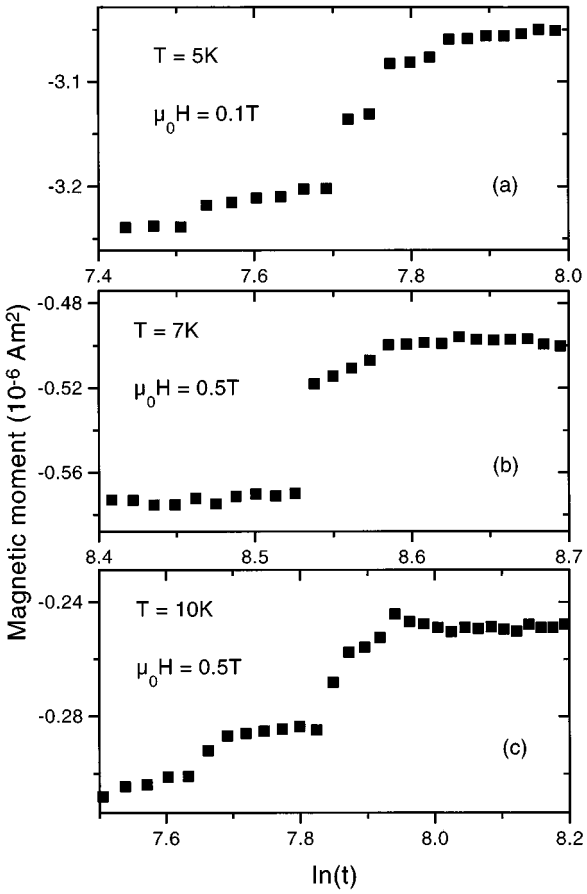

FIG. 11. Time-dependent magnetic moment during jumps in sample K1.

$$U_0 = \frac{k_b T}{S} \tag{9}$$

and is shown in the inset of Fig. 10. U_0 first increases with increasing temperature and then reaches a peak at some temperature T_m. This temperature T_m decreases almost linearly with increasing external fields.

We would like to point out that the temperature dependence of U_0 obtained from Eq. (9) is dependent on the initial magnetization M_0 used for the calculations. It is not possible to obtain the real values of M_0 from the experiment because the magnetization relaxes quite rapidly. Therefore, we have to use $M(t_0)$, which is recorded about 80 s after the stabilization of the magnetic field for the evaluation of the relaxation rate.

The magnetic relaxation obtained on samples K1, K2, and K3 with shielding fractions below 100% is completely different in character. The relaxation does not show a logarithmic behavior and jumps of the magnetization appear. Because the samples with 100% shielding fraction showed a very smooth logarithmic relaxation, we conclude that the unusual magnetic relaxation shown in Fig. 11 is an intrinsic property of samples with a nonideal shielding fraction. We wish to point out that a nonlogarithmic relaxation was also observed in powder samples (Refs. 22–24).

The height of the jumps increases with increasing magnetic field, but $M(t)$ becomes smoother with increasing temperature. The magnetic moment can decrease during the jumps by up to 15–20 % and this process may take some time as shown in Fig. 11 (note that every experimental point is taken 1 min after the other). We find either a set of small jumps [Fig. 11(a)] or one big jump, which is completed after several minutes of faster relaxation [Fig. 11(b)], or an alternation of slower and faster relaxations [Fig. 11(c)].

VII. SUMMARY

In the present contribution, the magnetic properties of single crystalline K_3C_{60} fullerene superconductors with shielding fractions from 25% to 100% were investigated. ac magnetic susceptibility measurements proved the absence of granularity for the supercurrents in the samples with 100% shielding fraction.

From dc magnetic measurements the upper critical field was determined and $\mu_0 H_{c2}(0)$ was found to be 28 T; the slope is $\delta\mu_0 H_{c2}/\delta T = -2.1$ T/K, close to T_c. No influence of the sample quality on H_{c2}(T) was found. The value of the coherence length at zero temperature is $\xi = 3.4$ nm. From ''trapped magnetic-moment'' measurements, the lower critical field was obtained and found to be $\mu_0 H_{c1}(0) = 1.2$ mT, and the penetration depth is $\lambda(0) = 870$ nm. The Ginzburg-Landau parameter for K_3C_{60} is $\kappa = 256$.

It was shown that the temperature dependence of both the coherence length and the penetration depth in the temperature range $0.78 \leqslant T < T_c$ can be well described by both BCS and Ginzburg-Landau theories. Arguments are presented that this dependence is better described by BCS theory at lower temperatures. The two-fluid model is found to be inappropriate.

The critical current density decreases smoothly with increasing temperature and external magnetic field. In a wide field range the magnetic field dependence of J_c is found to be proportional to $1/B$. The irreversibility line follows the power law $\mu_0 H_{\rm irr} = \mu_0 H_0 (1 - T/T_c)^{1.5}$.

A logarithmic time dependence of the magnetization is observed on samples with 100% shielding fraction. The relaxation rate at different magnetic fields increases progressively with temperature. The flux creep activation energy is found to be in the range from 10 to 80 meV with a peak in its temperature dependence. From measurements on samples with nonperfect stoichiometry we show that inhomogeneities strongly affect the relaxation process and may mask a logarithmic behavior.

ACKNOWLEDGMENTS

The authors are grateful to L. Pintschovius (INFP, Forschungszentrum Karlsruhe) for neutron-scattering measurements on sample K1. Work at the Atominstitut der Österreichischen Universitäten is supported by the Austrian Science Foundation (FWF) in part under Grant No. P12098-PHY and partly under Grant No. P11177-PHY, and at the Institut für Materialphysik under Grant No. P9741-PHY. Work at the University of Pennsylvania is supported by Department of Energy Grant No. DE-FC02-86ER45254.

[1] W. Krätschmer, L. D. Lamb, K. Fostiropoulos, and D. R. Huffman, Nature (London) **347**, 345 (1990).
[2] A. F. Hebard, M. J. Rosseinsky, R. C. Haddon, D. W. Murphy, S. H. Glarum, T. T. M. Palstra, A. P. Ramirez, and A. R. Kortan, Nature (London) **350**, 600 (1991).
[3] M. J. Rosseinsky, A. P. Ramirez, S. H. Glarum, D. W. Murphy, R. C. Haddon, A. F. Hebard, T. T. M. Palstra, A. R. Kortan, S. M. Zahurak, and A. V. Makhija, Phys. Rev. Lett. **66**, 2830 (1991).
[4] K. Tanigaki, I. Hirosawa, T. W. Ebbesen, J. Mizuki, Y. Shimakawa, Y. Kubo, J. S. Tsai, and S. Kuroshima, Nature (London) **356**, 419 (1992).
[5] K. Holczer, O. Klein, G. Grüner, J. D. Thompson, F. Diederich, and R. L. Whetten, Phys. Rev. Lett. **67**, 271 (1991).
[6] C. Politis, V. Buntar, W. Krauss, and A. Gurevich, Europhys. Lett. **17**, 175 (1992).
[7] G. Sparn, J. D. Thompson, R. L. Whetten, S.-M. Huang, R. B. Kaner, F. Diederich, G. Grüner, and K. Holczer, Phys. Rev. Lett. **68**, 1228 (1992).
[8] V. Buntar and H. W. Weber, Supercond. Sci. Technol. **9**, 599 (1996).
[9] M. Baenitz, M. Heinze, E. Straube, H. Werner, R. Schlögl, V. Thommen, H.-J. Güntherodt, and K. Lüders, Physica C **228**, 181 (1994).
[10] C. E. Johnson, H. W. Jiang, K. Holczer, R. B. Kaner, R. L. Whetten, and F. Diederich, Phys. Rev. B **46**, 5880 (1992).
[11] W. H. Wong, M. E. Hanson, W. G. Clark, G. Grüner, J. D. Thompson, R. L. Whetten, S.-M. Huang, R. B. Kaner, F. Diederich, P. Petit, J.-J. Andre, and K. Holczer, Europhys. Lett. **18**, 79 (1992).
[12] J. G. Hou, V. H. Crespi, X.-D. Xiang, W. A. Vareka, G. Briceno, A. Zettl, and M. L. Cohen, Solid State Commun. **86**, 643 (1993).
[13] A. P. Ramirez, Supercond. Rev. **1**, 1 (1994).
[14] J. D. Thompson, G. Sparn, K. Holczer, O. Klein, G. Grüner, R. B. Kaner, F. Diederich, and R. L. Whetten, in *Physical and Material Properties of High Temperature Superconductors*, edited by S. K. Malic and S. S. Shah (Nova, Commack, NY, 1994), p. 139.
[15] V. Buntar, U. Eckern, and C. Politis, Mod. Phys. Lett. B **6**, 1037 (1992).
[16] M. Kraus, H. Sindlinger, H. Werner, R. Schlögl, V. Thommen, H. P. Lang, H.-J. Gütherodt, and K. Lüders, J. Phys. Chem. Solids **57**, 999 (1996).
[17] Y. J. Uemura, A. Keren, L. P. Le, G. M. Luke, B. J. Sternlieb, W. D. Wu, J. H. Brewer, R. L. Whetten, S. M. Huang, S. Lin, R. B. Kaner, F. Diederich, S. Donovan, G. Grüner, and K. Holczer, Nature (London) **352**, 606 (1991).
[18] Y. J. Uemura, A. Keren, L. P. Le, G. M. Luke, W. D. Wu, J. S. Tsai, K. Tanigaki, K. Holczer, S. Donovan, and R. L. Whetten, Physica C **235-240**, 2501 (1994).
[19] L. Degiorgi, P. Wachter, G. Grüner, S. M. Huang, J. Wiley, and R. B. Kaner, Phys. Rev. Lett. **69**, 2987 (1992).
[20] V. Buntar, Phys. Lett. A **184**, 131 (1993).
[21] V. Buntar and A. G. Buntar, Phys. Rev. B **51**, 1311 (1995).
[22] C. L. Lin, T. Mihalisin, M. M. Labes, N. Bykovetz, Q. Zhu, and J. E. Fischer, Solid State Commun. **90**, 629 (1994).
[23] M.-W. Lee, M.-F. Tai, and S.-C. Luo, Jpn. J. Appl. Phys., Part 1 **34**, 126 (1995).
[24] V. Buntar, F. M. Sauerzopf, H. W. Weber, M. Riccó, L. Cristofolini, and F. Bolzoni, in *Recent Advances in Chemistry and Physics of Fullerenes and Related Materials*, edited by K. M. Kadish and R. S. Ruoff (Pennington, NJ, 1997), p. 1021.
[25] V. Buntar, F. M. Sauerzopf, H. W. Weber, J. E. Fischer, H. Kuzmany, M. Haluska, and C. L. Lin, Phys. Rev. B **54**, 14 952 (1996).
[26] V. Buntar, F. M. Sauerzopf, and H. W. Weber, Phys. Rev. B **54**, R9651 (1996).
[27] These approximations were done using a program developed by S. Kolesnik, which was based on an equation from J. A. Osborn, Phys. Rev. **67**, 351 (1945). The demagnetizing factor for sample K6, obtained from this calculation, was 0.139–0.17. From the initial slope in the Meissner phase D was found to be 0.14–0.148.
[28] G. S. Boebinger, T. T. M. Palstra, A. Passner, M. J. Rosseinsky, D. W. Murphy, and I. I. Muzin, Phys. Rev. B **46**, 5876 (1992).
[29] G. Sparn, J. D. Thompson, S.-M. Huang, R. B. Kaner, F. Diederich, R. L. Whetten, G. Grüner, and K. Holczer, Science **252**, 1829 (1991).
[30] N. R. Werthamer, E. Helfand, and P. C. Hohenberg, Phys. Rev. **147**, 295 (1966).
[31] T. T. M. Palstra, R. C. Haddon, A. F. Hebard, and J. Zaanen, Phys. Rev. Lett. **68**, 1054 (1992).
[32] S. C. Erwin and W. E. Pickett, Science **254**, 842 (1991).
[33] *Anisotropy Effects in Superconductors*, edited by H. W. Weber (Plenum Press, New York, 1977).
[34] C. Politis, A. I. Sokolov, and V. Buntar, Mod. Phys. Lett. B **6**, 351 (1992).
[35] V. Buntar, M. Ricco, L. Cristofolini, H. W. Weber, and F. Bolzoni, Phys. Rev. B **52**, 4432 (1995).
[36] V. Moshchalkov, J. V. Henry, C. Marin, J. Rossat-Mignod, and J. F. Jacquot, Physica C **175**, 407 (1991).
[37] C. Böhmer, G. Brandstätter, and H. W. Weber, Supercond. Sci. Technol. **10**, A1 (1997).
[38] A. I. Sokolov, Yu. A. Kufaev, and E. B. Sonin, Physica C **212**, 19 (1993).
[39] C. Politis, V. Buntar, and V. P. Seminozhenko, Int. J. Mod. Phys. B **7**, 2163 (1993).
[40] C. P. Bean, Phys. Rev. Lett. **8**, 250 (1962).
[41] R. D. Boss, J. S. Briggs, E. W. Jacobs, T. E. Jones, and P. A. Mosier-Boss, Physica C **243**, 29 (1995).
[42] S. H. Irons, J. Z. Liu, P. Klavins, and R. N. Shelton, Phys. Rev. B **52**, 15 517 (1995).
[43] S. Chu and M. E. McHenry (unpublished).
[44] F. M. Sauerzopf, H. P. Wiesinger, W. Kritscha, H. W. Weber, G. W. Crabtree, and J. Z. Liu, Phys. Rev. B **43**, 3091 (1991).
[45] Y. Yeshurun and A. P. Malozemoff, Phys. Rev. Lett. **60**, 2202 (1998).
[46] E. Zeldov, D. Majer, M. Konczykowski, V. Geskenbein, V. Vinokur, and H. Shtirkman, Nature (London) **375**, 373 (1995).
[47] M. R. Beasley, R. Labush, and W. W. Webb, Phys. Rev. **181**, 682 (1969).